High-temperature phase transitions in tungsten trioxide - the last word?

2002 J. Phys.: Condens. Matter 14 377

(http://iopscience.iop.org/0953-8984/14/3/308)

INSTITUTE OF PHYSICS PUBLISHING JOURNAL OF PHYSICS: CONDENSED MATTER

J. Phys.: Condens. Matter **14** (2002) 377–387 PII: S0953-8984(02)29010-4

High-temperature phase transitions in tungsten trioxide—the last word?

Christopher J Howard[1], **Vittorio Luca**[1] **and Kevin S Knight**[2]

[1] Materials Division, Australian Nuclear Science and Technology Organisation, Private Mail Bag 1, Menai, NSW 2234, Australia
[2] ISIS Facility, Rutherford Appleton Laboratory, Chilton, Didcot, Oxfordshire OX11 0QX, UK

E-mail: cjh@ansto.gov.au, vlu@ansto.gov.au and K.S.Knight@rl.ac.uk

Received 21 September 2001, in final form 31 October 2001
Published 21 December 2001
Online at stacks.iop.org/JPhysCM/14/377

Abstract

The structures of tungsten trioxide, WO_3, have been studied in fine temperature steps, from room temperature to 1000 °C, by means of very high-resolution neutron powder diffraction. It was confirmed that the sample used was single-phase monoclinic in space group $P2_1/n$ at room temperature. In addition to this monoclinic structure, the structures observed were an orthorhombic structure in $Pbcn$ from about 350 to 720 °C, another monoclinic structure in $P2_1/c$ from about 720 to 800 °C, a tetragonal structure in space group $P4/ncc$ from 800 to 900 °C, and above 900 °C a second tetragonal structure in $P4/nmm$. The transformation from the $Pbcn$ orthorhombic to the $P2_1/c$ monoclinic structure was certainly discontinuous, and indeed just above 720 °C two-phase mixtures were observed. The other transitions were continuous or nearly so, all three being apparently tricritical in nature. The sequence of phases, and nature (continuous or otherwise) of the transitions between them, can be well understood by reference to the results from a group theoretical analysis.

1. Introduction

Tungsten trioxide, WO_3, given its simple stoichiometry, adopts a surprising number of distinct crystalline forms [1–3]. All the polymorphs are three-dimensional networks of corner-linked WO_6 octahedra, and the majority, those comprising four-membered rings of the WO_6 octahedra, can be described as distorted variants of the cubic ReO_3 crystal structure. These distorted ReO_3-type structures can also be considered as variants of the perovskite, ABX_3, structure, in which the A-site cation is not just undersized but absent. For perovskites with undersized A cations, three different types of distortion have been identified [4, 5]: distortions of the BX_6 octahedral units, B-cation displacements within these octahedra, and the tilting of the corner-linked octahedral units relative to one another. Given the extreme circumstance of a missing A-site cation, it is not so surprising that WO_3 can form seven or more different perovskite-like structures involving distortions of all three types.

There have been a number of studies of WO_3 crystallography, motivated at least in part by the interesting physical properties and potential technological application of this material. WO_3 is a ferroelectric insulator at low temperatures, and a semiconductor at higher temperatures [6, 7]. Abrupt changes in volume, resistivity, and colour at temperature-induced phase transitions are also matters of interest [8, 9]. Superconductivity to 3 K has been observed along the domain walls in the slightly reduced oxide, WO_{3-x} ($x \sim 0.1$) [10], and nearly stoichiometric WO_3 has been considered an ideal material in which to investigate the behaviour of polarons [11]. As to its technological importance, WO_3 seems to be the favoured active material in electrochromic applications ('smart windows'), these depending on the colour change resulting from the voltage-driven intercalation of Li^+ ions into the structure [12]. Similarly, changes in electrical resistivity on intercalation of certain gases give rise to applications in gas sensors [13]. Tungsten trioxide represents the framework structure in the tungsten bronzes, and the perovskite-like bronzes such as Na_xWO_3 ($x \geqslant 0.25$) show interesting physical properties, including superconductivity, in their own right.

The history of WO_3 crystallography began with a room temperature x-ray single crystal study by Braekken [14] some 70 years ago. Braekken presented a triclinic structure, with an antiferroelectric pattern of cation displacements, but it was later argued [15] that the same structure could be described as monoclinic. Measurements made in the 1950s, on such properties as specific heat, thermal expansion, optical absorption, resistivity, and x-ray lattice parameters, revealed a number of phase transitions, especially at elevated temperatures. Sawada [8], for example, reports specific heat anomalies at 330, 740, 910 °C and a possible weak anomaly at 1230 °C. Among the best lattice parameters from that decade are those given by Perri *et al* [16]. These showed the structure of WO_3 to be monoclinic to about 330 °C, orthorhombic from this temperature up to a first-order transition at about 740 °C, and finally tetragonal to 1000 °C. Sawada [9] observed lattice parameter anomalies, but no change in symmetry at the higher-temperature transitions. On the basis of x-ray powder diffraction, Kehl *et al* [17] suggested a structure for the high-temperature tetragonal phase(s): space group $P4/nmm$, unit cell $a = 5.25$ Å, $c = 3.91$ Å, and displacements of the W atoms within the octahedra, alternately up and down the z-axis, giving an antiferroelectric pattern, similar to that proposed for Braekken's triclinic structure. It will prove convenient to refer unit-cell dimensions to those of the cubic (ReO_3-type) aristotype—so we will describe this structure as being in space group $P4/nmm$ on an (approximately) $\sqrt{2} \times \sqrt{2} \times 1$ unit cell. An impressive contribution on the structures near and below room temperature was made by Tanisaki. Tanisaki [18, 19] reported the existence of three phases: a low-temperature monoclinic phase to about −40 °C, a triclinic phase from about −40 to 17 °C, and a 'room temperature' monoclinic phase from 17 to about 350 °C, and using x-ray diffraction from a monodomain single crystal determined the structure of the room temperature monoclinic phase. This structure, in space group $P2_1/n$, on a $2 \times 2 \times 2$ ($\beta \approx 90°$) unit cell, was characterized again by an antiferroelectric pattern of cation displacements. Tanisaki's results have been generally confirmed in subsequent studies, although it turns out [20, 21] that at room temperature (∼20 °C) WO_3 can be found in either triclinic or monoclinic forms, or a mixture of both, depending on details of preparation including whether the sample has been ground, on crystallite size, and on thermal history. Tanisaki's monoclinic structure, in $P2_1/n$, has been verified in several studies by neutron powder diffraction [3, 22, 23], and the structures of the lower-temperature phases, monoclinic in space group Pc and triclinic in $P\bar{1}$, have been also determined [21, 24, 25]. Salje and Viswanathan [20] carried x-ray studies on WO_3 through to higher temperatures, into the orthorhombic phase, and suggested space group $Pmnb(Pnma)$ on a $2 \times 2 \times 2$ cell for the structure of this phase; the coordinates were given from a subsequent x-ray examination of a (twinned) crystal [26].

The year 1999 saw the appearance of four new publications on the high-temperature structures of WO_3, three reporting results from neutron powder diffraction [2, 3, 27] and the fourth [28] recording x-ray lattice parameters. Vogt *et al* [2] recorded neutron diffraction patterns at seven temperatures from 300 to 850 °C, and presented structures for monoclinic, orthorhombic, and tetragonal phases. In effect, they confirmed Tanisaki's structure [19] for the monoclinic phase, but disputed Salje's structure [26] for the orthorhombic phase—they proposed instead a structure in space group $Pbcn$. For the tetragonal phase to 850 °C they proposed a structure in $P4/ncc$ ($\sqrt{2} \times \sqrt{2} \times 2$ unit cell). Locherer *et al* [27] reported independently on structures in the tetragonal phase(s), both above and below the specific heat anomaly at 910 °C. Above this temperature (at 927 °C) they confirmed the early $P4/nmm$ structure of Kehl *et al* [17], whereas below this temperature (at 827 °C) they reported the same $P4/ncc$ tetragonal structure as was given by Vogt *et al* [2]. The $P4/ncc$ tetragonal structure differs from that in $P4/nmm$ only by small displacements of the oxygen atoms, a difference not detected in the x-ray studies [17]. Locherer *et al* [3, 27] reported lattice parameters derived from neutron powder patterns at some 37 temperatures ranging from 116 to 937 °C, though they did not take the opportunity to test all the structures. X-ray lattice parameter data were also reported [28].

In this paper we report the results from a new study of WO_3, from room temperature to 1000 °C in fine intervals of temperature, using very high-resolution neutron powder diffraction. As a preliminary, the most probable structures were identified from a group theoretical analysis. Our study confirms, *inter alia*, that the orthorhombic phase has the structure proposed by Vogt *et al* and also reveals a monoclinic phase existing from 720 to 790 °C, never previously recognized, yet critical to understanding why the transition at around 720 °C should be discontinuous. Comprehensive lattice parameter data are presented.

2. Group theoretical preliminaries

The high-temperature structure, tetragonal in $P4/nmm$, differs from the cubic aristotype in $Pm\bar{3}m$ by displacements of the W atoms, alternately parallel and anti-parallel to the z-axis. This antiferroelectric pattern of cation displacements seems to be preserved in the lower-symmetry structures (at least down to room temperature), the lower symmetries being associated with tilting of the corner-linked WO_6 octahedral units.

A full analysis of corner-linked tilting in perovskites, without cation displacement, has been given previously by Howard and Stokes [29]. The relevant irreducible representations (irreps) of the parent space group $Pm\bar{3}m$ were (in the notation of Miller and Love [30]) R_4^+ ($\boldsymbol{k} = 1/2, 1/2, 1/2$), corresponding to modes with out-of-phase tilting of octahedra in successive layers, and M_3^+ ($\boldsymbol{k} = 1/2, 1/2, 0$) associated with in-phase octahedral tilting. The analysis was completed using the computer program ISOTROPY[3].

Antiferroelectric patterns of cation displacement on the {100} planes of the cubic aristotype, as evidently occur in WO_3, can be recognized as transforming according to the irreducible representation M_3^- ($\boldsymbol{k} = 1/2, 1/2, 0$) of the parent space group $Pm\bar{3}m$. The different possible structures produced by M_3^--cation displacements followed by M_3^+ and R_4^+ octahedral tilting have been examined, again using the computer program ISOTROPY. The details are to be presented elsewhere [31]. Possible structures relevant to this work are presented in figure 1—the highest-symmetry space group shown in figure 1, $P4/nmm$, is that subgroup of $Pm\bar{3}m$ leaving invariant a structure with a single M_3^- distortion, and only subgroups of this space group have been included in the figure. The figure includes a description of the tilt

[3] ISOTROPY is a software package developed by Stokes and Hatch at Brigham Young University. ISOTROPY is available at www.physics.byu.edu/~stokesh/isotropy.html.

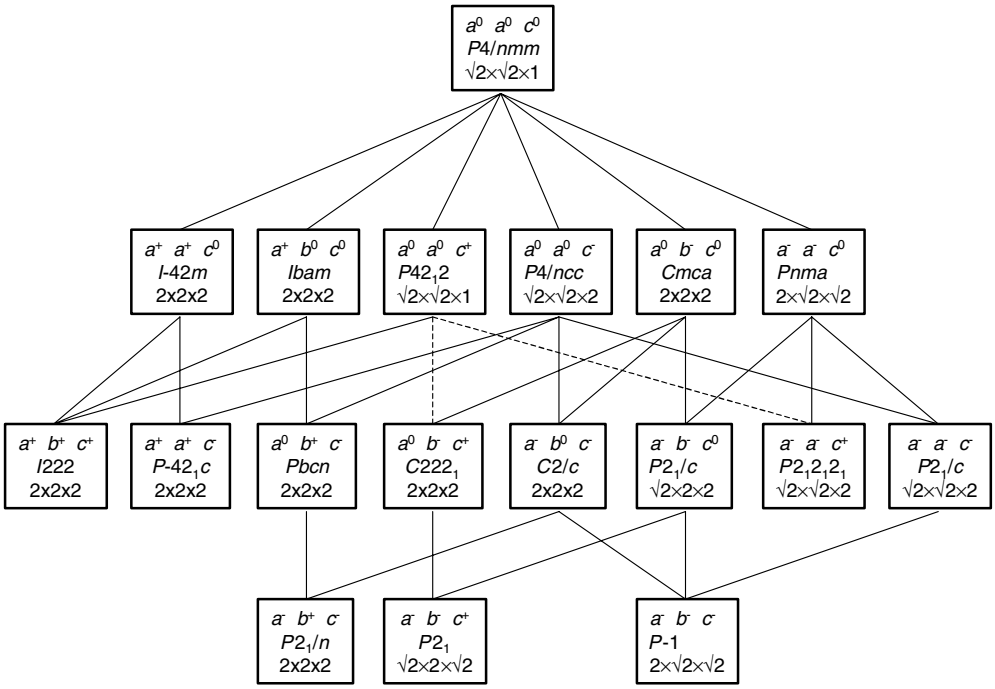

Figure 1. A schematic diagram indicating group–subgroup relationships among eighteen space groups considered relevant to this work. The corresponding structures are generated by an antiferroelectric pattern of cation displacements, followed by octahedral tilting. The tilting pattern is indicated using Glazer's notation. The space group is shown along with its approximate dimensions in terms of the cell dimension of the $Pm\bar{3}m$ parent—angles not required to be 90° are approximately 90° except in the case of the structure $a^-b^-c^0$ (space group $P2_1/c$) where the monoclinic angle is approximately 135°. A dashed line joining a group with its subgroup indicates that the corresponding phase transition is required to be first order.

system in each structure using Glazer's notation—briefly, the symbol $a^{\#}b^{\#}c^{\#}$ is used to indicate no tilt, in-phase octahedral tilting, or out-of-phase octahedral tilting about the ⟨001⟩ axes of the parent ($Pm\bar{3}m$) perovskite by showing the superscript # as 0, +, or − respectively [5, 32].

It is interesting to re-examine the literature in the light of this analysis. The tetragonal structures in $P4/nmm$ and $P4/ncc$ are consistent with the group theoretical analysis, as is the continuous nature of the transition between them. The same can be said for the orthorhombic structure $Pbcn$, and the monoclinic structure in $P2_1/n$ seen at room temperature or just above. The structure proposed for the orthorhombic phase by Salje [26], in $Pnma$ on a $2 \times 2 \times 2$ cell, does not appear on figure 1 nor anywhere in the ISOTROPY output, so would appear unlikely. On the other hand, if we accept that the transition at around 720 °C is from the $Pbcn$ structure to that in $P4/ncc$, it is a difficult to understand why it should be so markedly discontinuous. The structure analyses presented here have been assisted by reference to the results from ISOTROPY, as embodied in figure 1.

3. Experimental procedure

Diffraction patterns were recorded using the high-resolution neutron powder diffractometer, HRPD, at the ISIS facility, Rutherford Appleton Laboratories (RAL) [33]. The powdered sample of WO_3 was prepared by heating (Aldrich) tungstic acid in air at 1000 °C for 2 h, then

cooling to room temperature at 10 °C min^{-1}. X-ray diffraction indicated that the sample was single-phase monoclinic. About 5 g of the sample was loaded into an 11 mm diameter vanadium can, which was then mounted in the RAL vacuum furnace. This furnace has vanadium heating elements, the thermometry is based on type-K thermocouples positioned in contact with the sample can at about 20 mm above beam centre, and the sample temperature was controlled to ±0.2 K. Diffraction patterns were recorded from the sample at the 1 m position, in the back-scattering detector bank, over the time-of-flight range 30–130 ms, corresponding to d-spacings from 0.6 to 2.6 Å. The instrumental resolution in patterns so collected is $\Delta d/d \approx 4 \times 10^{-4}$, independent of d. The patterns were normalized to the incident beam spectrum as recorded in the upstream monitor, and corrected for detector efficiency according to prior calibration with a vanadium scan. Patterns were recorded first at room temperature, then in 20 ° steps from 100 to 300 °C, in 10 ° steps to 400 °C, in 20 ° steps to 640 °C, in 10 ° steps to 760 °C, in 20 ° steps to 860 °C, in 10 ° steps to 960 °C, and finally at 980 and 1000 °C. These temperatures were chosen to provide finer (10 °C) temperature steps near where phase transitions were previously reported. Most patterns were recorded to a total incident proton beam of 15 μA h, for approximately 20 min, which was sufficient to give a good determination of the lattice parameters. At room temperature, 500, 800, and 950 °C, longer counting times in the range 35–70 μA h incident beam were employed, so as to allow good structure determinations in the different phases—at these four temperatures data from the 90° detector bank, over the time-of-flight range 35–110 ms, corresponding to d-spacings from 1.0 to 3.2 Å were also recorded.

The different phases were identified from inspection of the diffraction patterns, along with reference to figure 1, as required. This process will be described in greater detail below. The identifications were confirmed, and both lattice parameters and atomic coordinates determined, using the Rietveld method as implemented in the GSAS computer program [34]. GSAS was used to fit the data from the back-scattering detector bank, and simultaneously to fit the data from the 90° detector bank when those also were recorded. Releasing the diffractometer constant for the 90° detector bank ensured that the lattice parameters were determined by the back-scattering data in every case. Internal coordinates were better determined when both data sets were recorded; however, only for the higher-symmetry structures could the refinement of a full set of anisotropic displacement parameters be supported.

4. Results and discussion

The diffraction patterns recorded at several temperatures, one in each of the five phases identified in our work, are shown in part in figure 2. This figure includes calculated patterns following analysis by the Rietveld method, assuming structures in the five different phases involved. The details of the structures of the five different phases, as determined by the Rietveld method, are recorded in table 1. In figure 2, the main peaks have been marked using indices based on a cell corresponding to the unit cell of the cubic aristotype (ReO_3), known as the 'pseudo-cubic cell' [4]. These peaks show splitting resulting from distortion of this cell—for example, the 200 reflection of the cubic cell shows as a well resolved 200/002 pair in the tetragonal structures at 800 and 950 °C, and as a resolved 200/020/002 triplet in the orthorhombic structure at 500 °C. Superlattice peaks have been marked according to their origin—those from the antiferroelectric cation displacements, characterized by half-integral h and/or k (on the pseudo-cubic cell) are marked AFE, those from out-of-phase octahedral tilting, with half-integral indices, are marked R, and those from in-phase octahedral tilting, having one integral and two half-integral indices, are marked M. We shall make reference to these indicated features, as well as to figure 1, in the discussion to follow.

As mentioned above, measurements were made first at room temperature, then at

Table 1. Details of five structures of WO_3. Anisotropic displacement parameters, U_{ij}, are given in units of 10^{-2} Å^2. The number in parentheses beside each entry indicates the estimated standard deviation referred to the last figure shown.

Atom	x	y	z	U_{11}	U_{22}	U_{33}	U_{12}	U_{13}	U_{23}
$T = 20\,^\circ$C, space group $P2_1/n$, $a = 7.3033(2)$ Å, $b = 7.5375(2)$ Å, $c = 7.6920(2)$ Å, $\beta = 90.855(1)^\circ$									
W_1	0.2528(6)	0.0260(7)	0.2855(4)	−0.3(1)	−0.3	−0.3	0.0	0.0	0.0
W_2	0.2497(6)	0.0341(6)	0.7805(5)	0.0(1)	0.0	0.0	0.0	0.0	0.0
O_1	0.0003(6)	0.0337(7)	0.2122(4)	0.3(1)	0.3	0.3	0.0	0.0	0.0
O_2	−0.0011(7)	0.4632(8)	0.2177(5)	0.8(1)	0.8	0.8	0.0	0.0	0.0
O_3	0.2843(3)	0.2598(7)	0.2852(3)	0.5(1)	0.5	0.5	0.0	0.0	0.0
O_4	0.2080(4)	0.2588(8)	0.7332(3)	0.8(1)	0.8	0.8	0.0	0.0	0.0
O_5	0.2856(5)	0.0410(4)	0.0041(4)	0.4(1)	0.4	0.4	0.0	0.0	0.0
O_6	0.2841(5)	0.4868(4)	−0.0056(3)	0.5(1)	0.5	0.5	0.0	0.0	0.0
$T = 500\,^\circ$C, space group $Pcnb$, $a = 7.3572(1)$ Å, $b = 7.5735(1)$ Å, $c = 7.7607(1)$ Å									
W	0.2514(3)	0.0293(2)	0.2828(1)	1.05(4)	1.05	1.05	0.00	0.00	0.00
O_1	−0.0020(5)	0.0319(1)	0.2239(1)	0.66(7)	2.08(6)	2.70(7)	−1.1(1)	−0.2(1)	−0.1(1)
O_2	0.2828(1)	0.2571(3)	0.2578(2)	2.06(6)	1.22(7)	4.07(8)	0.4(1)	−0.2(1)	0.4(1)
O_3	0.2786(1)	0.0124(3)	0.0040(1)	2.42(7)	4.04(8)	0.94(7)	−0.3(2)	−0.3(1)	0.1(1)
$T = 760\,^\circ$C, space group $P2_1/c$, $a = 5.2793(2)$ Å, $b = 5.2635(2)$ Å, $c = 7.8329(2)$ Å, $\beta = 90.483(1)^\circ$									
W	0.2466(11)	0.2518(17)	0.7169(6)	1.8(1)	1.8	1.8	0.0	0.0	0.0
O_1	0.2516(16)	0.2796(12)	−0.0051(7)	5.3(3)	5.0(4)	1.6(3)	1.6(7)	0.5(2)	0.5(6)
O_2	0.0341(21)	−0.0268(25)	0.7633(18)	1.9(5)	3.0(5)	5.4(5)	−1.6(4)	−0.3(3)	0.1(4)
O_3	0.5261(21)	0.0318(16)	0.7654(18)	2.1(5)	2.3(4)	4.3(5)	0.8(4)	−0.2(3)	−0.1(4)
$T = 800\,^\circ$C, space group $P4/ncc$, $a = 5.2772(1)$ Å, $c = 7.8486(1)$ Å									
W	1/4	1/4	0.2843(1)	2.25(5)	2.25(5)	1.10(8)	0	0	0
O_1	1/4	1/4	0.0028(1)	5.32(6)	5.32(6)	1.51(8)	0	0	0
O_2	0.0289(1)	−0.0289(1)	1/4	2.17(4)	2.17(4)	5.47(7)	−1.06(4)	−0.09(4)	−0.09(4)
$T = 950\,^\circ$C, space group $P4/nmm$, $a = 5.2970(1)$ Å, $c = 3.9294(1)$ Å									
W	1/4	1/4	−0.0679(3)	2.39(6)	2.39(6)	1.38(8)	0	0	0
O_1	1/4	1/4	0.4953(3)	5.95(6)	5.95(6)	1.75(9)	0	0	0
O_2	0	0	0	3.54(4)	3.54(4)	6.09(8)	−2.20(5)	0.16(4)	0.16(4)

successively higher temperatures up to a maximum of 1000 °C. For the purposes of this discussion, however, it is convenient to consider the structures in reverse order, starting with the highest-symmetry structure as observed at the highest temperatures.

The pattern recorded at 950 °C is the simplest of the patterns recorded, and represents the structure with the highest symmetry. The splitting of the (pseudo-cubic) 200 from the 002 is indicative of tetragonal splitting. Only AFE superlattice reflections are seen—there is no evidence for any octahedral tilting. Thus the tilt system is $a^0a^0c^0$; and the space group is $P4/nmm$. This is the tetragonal structure first proposed by Kehl *et al* [17], and confirmed in the recent study by Locherer *et al* [27].

Below 900 °C, the neutron diffraction patterns show additional peaks, just two of these being seen in that part of the 800 °C diffraction pattern shown in figure 2. The indices of these additional reflections, referred to the pseudo-cubic cell, are $\frac{3}{2}\,\frac{1}{2}\,\frac{3}{2}$ ($d \approx 1.75$ Å) and $\frac{3}{2}\,\frac{1}{2}\,\frac{1}{2}$ ($d \approx 2.27$ Å). Evidently, both reflections can be attributed to R-point distortions, that is to an out-of-phase pattern (superscript − in Glazer's notation) of octahedral tilting. In fact the analysis of octahedral tilting can be taken further, since according to Glazer (in 1975) the appearance of R-point reflections with $h \neq k$, along with the absence of corresponding $h = k$

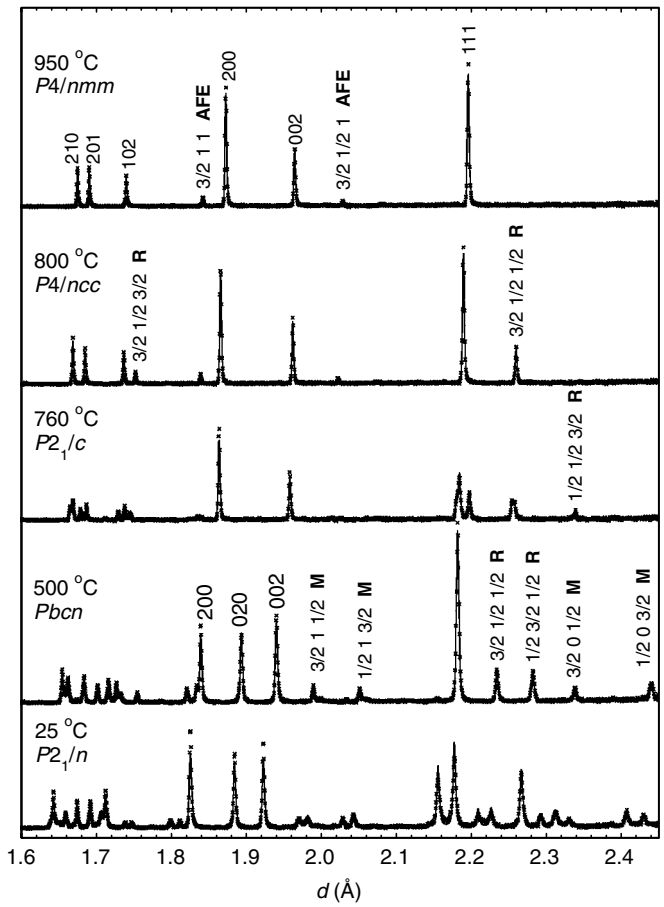

Figure 2. The observed diffraction patterns (crosses) from WO_3 in each of its five high-temperature phases, the reflections being marked as fundamental perovskite reflections or superlattice reflections arising from antiferroelectric cation displacements and/or octahedral tilting. The continuous curves are fits obtained by the Rietveld method assuming structures in the space groups indicated. The significance of the splitting of the fundamental peaks and the presence or absence of superlattice reflections is explained in the text.

reflections (such as the $\frac{1}{2}\,\frac{1}{2}\,\frac{3}{2}$ ones, $d \approx 2.34$ Å), implies that only around the c-axis does tilting occur. The tilt system must be $a^0a^0c^-$, and the space group $P4/ncc$. The structure is that reported by Vogt *et al* [2] and independently by Locherer *et al* [27]. Despite early reports of both specific heat and lattice parameter anomalies near 900 °C [9, 17], not until the application of neutron diffraction in 1999 was this structure distinguished from the higher-symmetry structure of the previous paragraph. The R-point reflections are entirely due to small displacements of the oxygen atoms (resulting from tilting of the WO_6 octahedra), and though they can be very easily seen in the neutron diffraction pattern of figure 2, they have not been seen with x-rays.

Just below 800 °C, we observed a broadening of the 111 reflection which, at the very high resolution used, was seen as a splitting at lower temperatures. The pattern recorded at 760 °C is included in figure 2. The patterns recorded at temperatures from 750 to 790 °C showed monoclinic distortion, reflected in the broadening or splitting of the pseudo-cubic 111 reflection, but no reflections that would indicate a larger unit cell. Taking these observations along with the continuous nature of the transition from this phase to the tetragonal $P4/ncc$

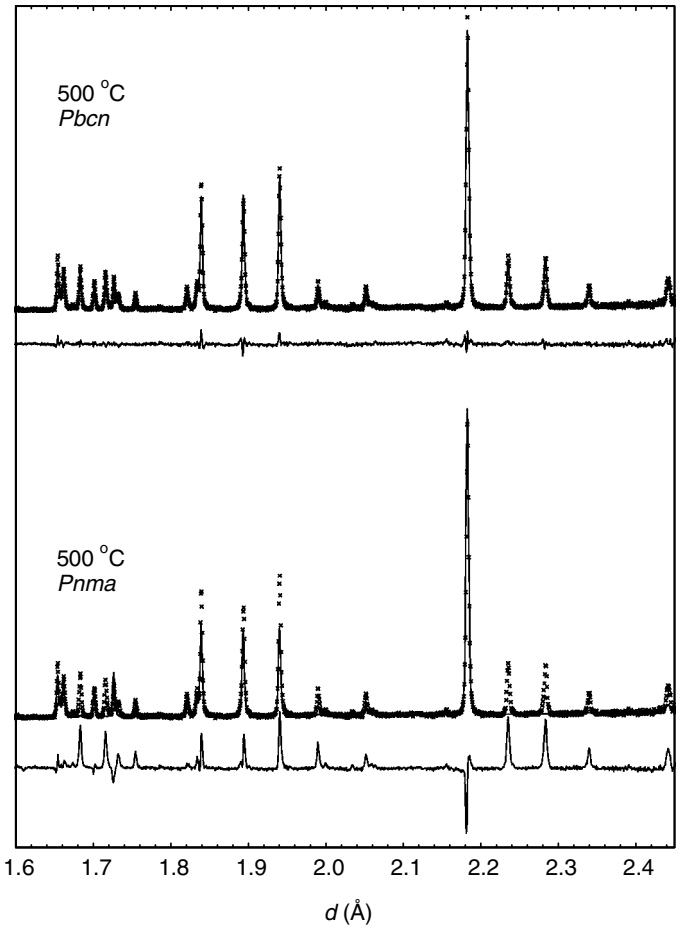

Figure 3. A test of the models proposed for the orthorhombic phase by Vogt *et al* [2] (space group $Pbcn$) and Salje [26] (space group $Pnma$). The figure shows the observed pattern (crosses) and the best fit obtained in each case (continuous curve through the pattern). The continuous curve, below each pattern, represents the difference between the observed pattern and the calculated one.

phase, and referring to figure 1, it can be concluded that the space group of this hitherto unreported phase is $P2_1/c$, tilt system $a^-a^-c^-$. Consistent with this assignment, because it implies out-of-phase octahedral tilting around a second axis, is the appearance of the previously absent R-point reflection at $\frac{1}{2}\,\frac{1}{2}\,\frac{3}{2}$ ($d = 2.34$ Å). Initial estimates of the atomic coordinates were obtained using ISOTROPY, and these estimates were refined using the Rietveld method as implemented in GSAS. The refined coordinates are included in table 1, and the corresponding fit of the calculated pattern to that observed is shown (in part) in figure 2. This monoclinic phase is observed over a limited temperature range, from about 720 to 790 °C, though it occurs as a pure single phase only from about 750 °C. Though ours is the first identification of this new monoclinic phase, it is notable that Kehl *et al* [17] commented on broadening of lines in the back-reflection region of patterns recorded in this temperature range, while at similar temperatures there is a 40 °C gap in the lattice parameter data of Locherer *et al* [3,27]. Vogt *et al* [2] took no measurements at temperatures where this monoclinic phase might have been found.

Between 350 and 720 °C the structure is orthorhombic. The pseudo-cubic 200/020/002

reflections are well separated, whereas the 111 reflection is again a single sharp peak. The diffraction patterns show both R- and M-point reflections. As mentioned earlier, two distinct orthorhombic structures have been proposed, both on a $2 \times 2 \times 2$ unit cell—one in space group $Pnma$ [26] and the other in $Pbcn$ [2]. It was concluded from the group theoretical analysis that the second structure is to be preferred, and this conclusion is confirmed by comparing the fits to the data obtained for the two models proposed (figure 3). It is interesting to note that the same $Pbcn$ structure would be suggested by a closer analysis of the superlattice reflections. The R-point reflection $\frac{1}{2}\ \frac{1}{2}\ \frac{3}{2}$, now expected at $d = 2.32$ Å, seems to have disappeared, and the only M-point reflections appearing are those with integral k. This implies [5] that out-of-phase tilts (− in Glazer notation) occur only around the c-axis, and in-phase tilts (+ in Glazer notation)

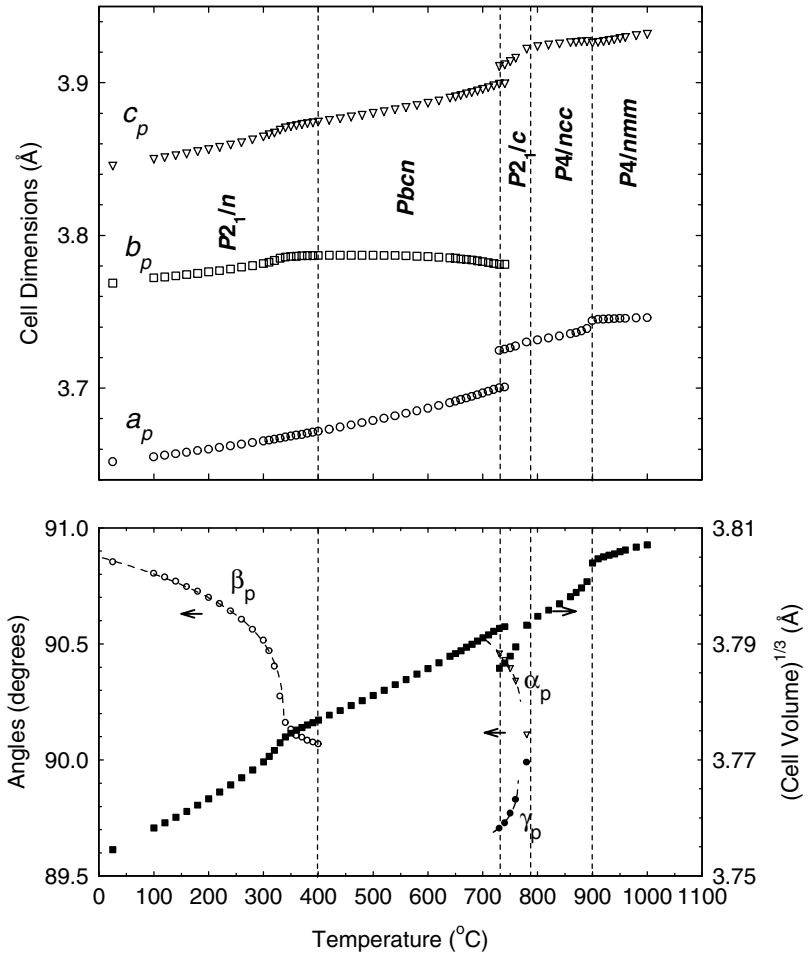

Figure 4. Temperature dependences of lattice parameters and cell volume for WO_3. The upper plot shows the lengths of the edges of the pseudo-cubic cell, and the lower plot the angles in this pseudo-cubic cell where these differ from 90°, as well as the cube root of the cell volume. The phase transition temperatures are indicated. At temperatures just above 720 °C, two values of each cell parameter are shown, reflecting the two-phase mixtures encountered near the first-order transition. The broken lines shown in the lower plot represent the expected variations of the angles on the basis that structural transitions, from each of these monoclinic structures to the orthogonal structures above them, are tricritical in nature.

only around the b-axis. Thus the tilt system is $a^0b^+c^-$ and (from figure 1) the structure is that in $Pbcn$. The transition from orthorhombic to the monoclinic $P2_1/c$ structure is characterized by sudden changes in lattice parameters (figure 4), and the occurrence of two-phase regions—it is first order as, given the absence of a group–subgroup connection (figure 1), the group theoretical analysis requires.

Below 350 °C, the 111 peak again develops splitting, indicating the occurrence of another monoclinic phase. This is the monoclinic structure in space group $P2_1/n$, tilt system $a^-b^+c^-$, just as determined by Tanisaki [19] more than 40 years ago. The sample that we used was single-phase monoclinic from room temperature, presumably because its preparation involved cooling from higher temperatures. The representative diffraction pattern shown in figure 2 is indeed that recorded at room temperature, and the details of the monoclinic structure recorded in table 1 are those derived from the pattern shown.

All patterns have been fitted assuming structures as indicated above, and precise lattice parameters obtained in every case. The evolution of the structure with temperature is best followed by showing the dimensions (cell edges, monoclinic angle) of the pseudo-cubic cell as a function of temperature (figure 4). The cube root of the volume of this cell is also displayed. It is apparent from this figure that the transition from the $Pbcn$ orthorhombic to the $P2_1/c$ monoclinic structure is discontinuous, with a volume decrease of 0.5%. Mixtures of the $Pbcn$ and $P2_1/c$ phases were observed in the vicinity of this transition, as is typical for first-order transitions. The other transitions appeared to be continuous, or at least very nearly so. Locherer *et al* quite carefully examined the transitions from monoclinic $P2_1/n$ to orthorhombic [3] and from tetragonal $P4/ncc$ to tetragonal $P4/nmm$ [27] structure, and concluded that both were tricritical in nature [35]. We concur with this conclusion, and suggest that the additional transition from monoclinic $P2_1/c$ to tetragonal $P4/ncc$ structure is also tricritical. We show in figure 4, for comparison with the experimental results, the expected variations with temperature in tricritical transitions of the monoclinic angle for the transitions from $P2_1/n$ and $P2_1/c$. The variation of the shorter cell edge parameter for the transition from $P4/ncc$ to $P4/nmm$ is also approximately as expected for a tricritical transition.

To summarize, we found our sample of WO_3 to be single-phase monoclinic at room temperature, and observed four phase transitions while heating it to 1000 °C. The sequence of structures in WO_3, starting from the monoclinic structure in space group $P2_1/n$, can be summarized in the following schematic diagram:

350 °C	720 °C	800 °C	900 °C

Monoclinic ------> Orthorhombic ------> Monoclinic ------> Tetragonal ------> Tetragonal

$P2_1/n$	$Pbcn$	$P2_1/c$	$P4/ncc$	$P4/nmm$
$a^-b^+c^-$	$a^0b^+c^-$	$a^-a^-c^-$	$a^0a^0c^-$	$a^0a^0c^0$
Continuous	Discontinuous	Continuous	Continuous	

We have in the course of this work confirmed the previously determined structures in space groups $P2_1/n$, $P4/ncc$, and $P4/nmm$. We have established that the orthorhombic structure is correctly described in space group $Pbcn$ [2]. A new intermediate monoclinic phase, in $P2_1/c$, has been identified for the first time, and its structure determined. For the sequence as now determined, the transitions are found to be continuous or discontinuous exactly as expected from the group theoretical analysis (refer figure 1). In particular, the occurrence of just one first-order transition is neatly explained by the occurrence of the newly identified $P2_1/c$ monoclinic phase—it would be difficult to understand (refer figure 1 again) why a sequence without this intermediate (as per [2]) should show any discontinuous transition at all. Since the results that we have obtained are based on neutron diffraction data of the highest

available resolution, and the sequence obtained is now entirely in accord with expectations from the group theoretical analysis, we believe that the sequence of structures obtained on heating WO_3 has at last been completely determined[4].

Acknowledgments

The authors thank Jonathan Widjaja for assistance with sample preparation and the preliminary checks by x-ray diffraction, and Professor Harold Stokes, of Brigham Young University, for contributions on the group theoretical analysis without which this work could not have been completed. Support for travel by VL and CJH from the Access to Major Research Facilities Programme is gratefully acknowledged.

References

[1] Labbe Ph 1992 *Key Eng. Mater.* **68** 293–339
[2] Vogt T, Woodward P M and Hunter B A 1999 *J. Solid State Chem.* **144** 209–15
[3] Locherer K R, Swainson I P and Salje E H K 1999 *J. Phys.: Condens. Matter* **11** 6737–56
[4] Megaw H D 1973 *Crystal Structures: a Working Approach* (Philadelphia, PA: Saunders) pp 285–302
[5] Glazer A M 1975 *Acta Crystallogr.* A **31** 756–62
[6] Sawada S and Danielson G C 1959 *Phys. Rev.* **113** 803–5
[7] Salje E 1976 *Ferroelectrics* **12** 215–17
[8] Sawada S 1956 *J. Phys. Soc. Japan* **11** 1237–46
[9] Sawada S 1956 *J. Phys. Soc. Japan* **11** 1246–52
[10] Aird A and Salje E K H 1998 *J. Phys.: Condens. Matter* **10** L377–80
[11] Schirmer O F and Salje E 1980 *J. Phys. C: Solid State Phys.* **13** L1067–72
[12] Granqvist C G 1999 *Electrochim. Acta* **44** 3005–15
[13] Wang X S, Miura N and Yamazoe N 2000 *Sensors Actuators* **66** 74–6
[14] Braekken H 1931 *Z. Kristallogr.* **78** 484–8
[15] Andersson G 1953 *Acta Chem. Scand.* **7** 154–8
[16] Perri J A, Banks E and Post B 1957 *J. Appl. Phys.* **28** 1272–5
[17] Kehl W L, Hay R G and Wahl D 1952 *J. Appl. Phys.* **23** 212–15
[18] Tanisaki 1960 *J. Phys. Soc. Japan* **15** 566–73
[19] Tanisaki 1960 *J. Phys. Soc. Japan* **15** 573–81
[20] Salje E and Viswanathan 1975 *Acta Crystallogr.* A **31** 356–9
[21] Woodward P M, Sleight A W and Vogt T 1995 *J. Phys. Chem. Solids* **56** 1305–15
[22] Loopstra B O and Boldrini P 1966 *Acta Crystallogr.* **21** 158–62
[23] Loopstra B O and Rietveld H M 1969 *Acta Crystallogr.* B **25** 1420–1
[24] Salje E K H, Rehmann S, Pobell F, Morris D, Knight K S, Herrmansdorfer T and Dove M T 1997 *J. Phys.: Condens. Matter* **9** 6563–77
[25] Diehl R, Brandt G and Salje E 1978 *Acta Crystallogr.* B **34** 1105–11
[26] Salje E 1977 *Acta Crystallogr.* B **33** 574–7
[27] Locherer K R, Swainson I P and Salje E H K 1999 *J. Phys.: Condens. Matter* **11** 4143–56
[28] Locherer K R and Salje E 1999 *Phase Transitions* **69** 85–93
[29] Howard C J and Stokes H T 1998 *Acta Crystallogr.* B **54** 782–9
[30] Miller S C and Love W F 1967 *Tables of Irreducible Representations of Space Groups and Co-Representations of Magnetic Space Groups* (Boulder, CO: Pruett)
[31] Stokes and Howard 2001 in preparation
[32] Glazer A M 1972 *Acta Crystallogr.* B **28** 3384–92
[33] Ibberson R M, David W I F and Knight K S 1992 *Rutherford Appleton Laboratory Report* RAL 92–031
[34] Larson A C and Von Dreele R B 1986 *GSAS* general structure analysis system *Los Alamos National Laboratory Report* LAUR 86–748
[35] Salje E K H 1990 *Phase Transitions in Ferroelastic and Co-elastic Crystals* (Cambridge: Cambridge University Press)

[4] A transition to the ReO_3 structure, in $Pm\bar{3}m$, might be expected to occur at higher temperatures. However, Sawada [9] reports that WO_3 remains tetragonal to 1280 °C, and probably to 1400 °C.